Charles University in Prague
Faculty of Mathematics and Physics

BACHELOR THESIS

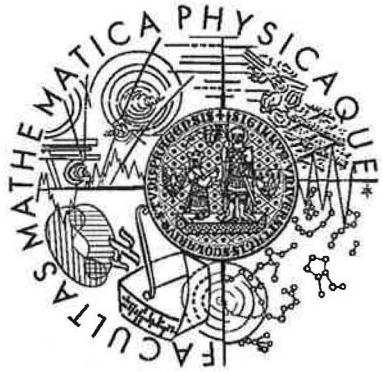

Petr Soukal

The Study of Jet Structure of ep Interactions with HZTOOL Method

Institute of Particle and Nuclear Physics

Supervisor: RNDr. Alice Valkárová, DrSc.
Specialization: Physics, General Physics

2007

I would like to thank my supervisor RNDr. Alice Valkárová, DrSc. for her invaluable help, uncomplainingness and guidance.

Prohlašuji, že jsem svou bakalářskou práci napsal samostatně a výhradně s použitím citovaných pramenů. Souhlasím se zapůjčováním práce.

V Praze dne

Petr Soukal

Contents

1 Overview **6**

1.1 Introduction to Diffraction 6

1.2 Kinematics of Diffractive Scattering 7

1.3 H1 detector description 8

1.4 Thrust jet analysis method 9

1.5 Monte Carlo generator RAPGAP 10

1.6 HZTool 11

2 Results **12**

3 Conclusion **16**

References **17**

Název práce: Studium jetové struktury ep difrakčních interakcí s pomocí metody HZTOOLs
Autor: Petr Soukal
Katedra (ústav): Ústav časticové a jaderné fyziky
Vedoucí bakalářské práce: RNDr. Alice Valkárová, DrSc.
e-mail vedoucího: alice@ipnp.troja.mff.cuni.cz

Abstrakt: V roce 1997 byla publikována analýza difrakčních eventů v hluboce nepružných *ep* srážkách, na datech získaných na detektoru H1 na HERA. Získané výsledky byly srovnány s několika Monte Carlo modely. Použitím knihovny HZTool jsou srovnána publikovaná experimentální data s výsledky generovanými novější verzí (z roku 2005) Monte Carlo modelu RAPGAP.

Klíčová slova: difrakce, HZTools, RAPGAP, hluboce nepružný rozptyl,*ep* interakce, thrust

Title: The Study of Jet Structure of ep Interactions with HZTOOL Method
Author: Petr Soukal
Department: Institute of Particle and Nuclear Physics
Supervisor: RNDr. Alice Valkárová, DrSc.
Supervisor's e-mail address: alice@ipnp.troja.mff.cuni.cz

Abstract: A thrust analysis of diffractive events in deep inelastic ep collision, using data taken by the H1 detector at HERA, has been published in 1997. The experimental results were compared with several Monte Carlo models. Using HZTool library, an attempt is made to compare the published experimental results with a newer version of the RAPGAP MC model from 2005.

Keywords: diffraction, HZTools, RAPGAP, deep inelastic scattering,*ep* interaction, thrust

Motivation

Diffraction is a very interesting physical process, no matter whether we consider the diffraction of light or of particles. Unlike the latter, the former is understood very well today and is described by valid laws of physics. The explanation of the latter, i.e. of the diffraction of "elementary" particles is attempted via Quantum Chromodynamics (QCD), by the Theory of Strong Interactions, which forms an integral part of the standard model. Unfortunately, even this theory fails to explain satisfactorily all processes occuring during particle diffraction, and even less their results.

After first years of data taking at HERA experiments, the Large Rapidity Gap events were observed which could be attributed mainly to diffraction. The diffraction is a process where the hadron (in our case of *ep* collision proton) must leave the collision site unaltered. In 1997 was published a paper [1] which analyses thrust.

Thrust is the quantity, which tells us about the measure of shape of events (if the shape is perfectly spherical then the thrust is equal to 0.5, if two particles travel in two opposite directions on one line, thrust is 1).

Another variable studied in [1],P_t^2, expresses the deflection of the main thrust axis of the emerging "particle jet" from the direction of the original proton. The larger this quantity is, the larger the deflection.

It was discovered that the used models do not describe the diffraction characteristics of events.

The comparison of published results and theoretical predictions is possible using HZTool. It is a library of routines which will allow us to reproduce an experimental result using the four-vector final state from Monte Carlo generators. This library involves data from HERA and TeVatron. So we can easily test how the measured and published data are described by the latest theoretical predictions and analyze, whether the new models have shown any improvement compared to the older ones.

The aim of this work is to compare the results of old Monte Carlo model used in [1] with the newer one. Here applied MC generator is RAPGAP,version 3.01 from 2005.

Chapter 1

Overview

1.1 Introduction to Diffraction

In hadron-hadron scattering, interactions are classified by the characteristics of the final states. In elastic scattering, both hadrons emerge unscathed and no other particles are produced. In diffractive scattering, the energy transfer between the two interacting hadrons remains small, but one (single dissociation) or both (double dissociation) hadrons dissociate into multi-particle final states, preserving the quantum numbers of the associated initial hadron. The remaining configurations correspond to inelastic interactions.

The first interpretation of diffraction, developed by Feinberg and Pomerunchuk [2] and Good and Walker [3], was that different components of the projectile were differently absorbed by the early indications of the composite nature of hadrons.

According to the Regge theory of strong interaction [4], diffraction originates form exchanging a universal trajectory with quantum numbers of the vacuum, the (soft) Pomeron $\mathbb{P}$, introduced by Gribov [5].

Within Quantum Chromodynamics, the candidate for vacuum exchange with properties similar to the soft Pomeron is two gluons exchange [6, 7]. As a result of interactions between the two gluons, a ladder structure develops. In perturbative QCD, the properties of this ladder depend on the energy and scales involved in the interaction, which means, that its character will be individual for different parameters. In the high-energy limit, the properties of the ladder have been derived for multi-Regge kinematics and the resulting exchange is called the (hard) BFKL Pomeron [8, 9, 10].

A renewed interest in diffractive scattering followed the observation of a copious production of diffractive-like events in deep inelastic scattering (DIS) at HERA ep collider [11, 12] as well as the earlier observation of jet production associated with a leading proton in $p\bar{p}$ at CERN [13]. The presence of a large scale opens the possibility of studying the partonic structure of the diffractive exchange as suggested by Ingelman and Schlein [14] and testing QCD dynamics. Moreover, studying diffractive scattering offers a unique opportunity to understand the relation between the fundamental degrees of freedom prevailing in soft interactions - hadrons and Regge

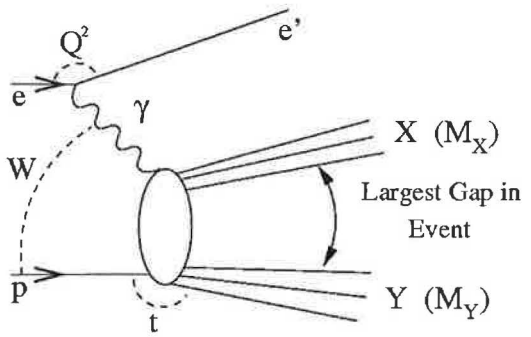

Figure 1.1: Ilustration of the process, $ep \to e'XY$, in which the hadron system X and Y are separated by the largest rapidity gap in event. W is the invariant mass of colliding virtual photon - beam proton system. $-Q^2$ is the square of the 4/momentum transfer at the (e,e') vertex, and t at the (p, Y) vertex. M_X and M_Y are the masses of systems X and Y, respectively.

trajectories, and those of QCD - quarks and gluons. Establishing both theoretically and experimentally the reactions in which the soft component is dominant and those in which the perturbative QCD formalism is applicable is one of the greatest challenges of this field of interest.

1.2 Kinematics of Diffractive Scattering

The variables used to analyze diffractive scattering will be introduced for ep DIS. Because DIS is considered as a two-step process in which the incoming lepton emits a photon which then interacts with the proton target, the relevant variables can be generalized easily to $p\bar{p}$ interactions. A diagram for diffractive scattering, where the diffracted state is separated from the scattered proton by a large rapidity gap (LRG), is presented in Fig. 1.1. All the relevant four vectors are defined therein. In addition to the usual DIS variables,

$$Q^2 = -q^2 = -(k - k')^2, \tag{1.1}$$
$$W^2 = (q + p)^2, \tag{1.2}$$
$$x = \frac{Q^2}{2p \cdot q}, \tag{1.3}$$
$$y = \frac{p \cdot q}{p \cdot k}, \tag{1.4}$$

the variables used to described the diffractive final state are,

$$t = (p - p')^2, \tag{1.5}$$
$$x_{\mathbb{P}} = \frac{q \cdot (p - p')}{q \cdot p} \simeq \frac{M_X^2 + Q^2}{W^2 + Q^2}, \tag{1.6}$$
$$\beta = \frac{Q^2}{2q \cdot (P - P')} = \frac{x}{x_{\mathbb{P}}} \simeq \frac{Q^2}{M_X^2 + Q^2}. \tag{1.7}$$

$x_{\mathbb{P}}$ is the fractional loss of the proton longitudinal momentum. It is sometimes denoted by ξ. β is the equivalent of Bjorken x, but relative to the exchanged object. M_X is the invariant mass of the hadronic final state recoiling against the leading proton $M_X^2 = (q + p - p')^2$. The approximate relations hold for small values of the four-momentum transfer squared t and large W, typical of high energy diffraction.

The need to have a clear identity of the target in diffractive scattering limits the square of the momentum transfer, $|t| < 1/R_T^2$, where R_T is the radius of the target. The t distribution typically behaves exponentially, $f(t) \sim \exp(-b|t|)$ with $b \simeq R_T^2/6$. The allowed M_X is also determined by the coherence requirements. The minimum value of t required to produce a given M_X from a target with mass m_T is $|t|_{\min} \simeq m_T^2(M_X^2 + Q^2)^2/W^4$. For a typical hadron radius of 1 fm, $M_X^2 < 0.2W^2$ and the hadronic final state exhibits a large rapidity gap between the fragments of the diffracted state and the unscathed target (see Fig. 2). This is why, in collider experiments, diffractive events are identified either by the presence of a fast proton along the beam direction or by the presence of large rapidity gap in the central detectors.

1.3 H1 detector description

Only detector components, which were part of detector in the year of taking data (1994), relevant to the analysis will be desribed. A detailed description of the H1 detector can be found elsewhere [15].

The "backwards"electromagnetic calorimeter (BEMC) covers th full azimuth, and extends over the range $151° < \theta < 176°$, where θ is the polar angle with respect to the proton beam direction, as seen from the nominal beam collision point. The BEMC was used to trigger on and measure the energy of the scattered electron in DIS processes. The electromagnetic energy resolution is $\sigma_E/E = 0.10/\sqrt{E\,[GeV]} \oplus 0.42/E[GeV] \oplus 0.03$ [16], while the absolute electromagnetic energy scale is known with an accuracy of 1 %. The BEMC hadronic energy is known to the precision of 20 %.

The LAr calorimeter is placed inside a superconducting solenoid providing a steady and homogeneous magnetic field of 1.15 T parallel to the beam axis in the tracking region. The track reconstruction is based on the information from the central jet chamber (CJC), the z-drift chambers and the forward tracker. These detectors cover a polar angular range of $5° < \theta < 155°$.

Forward energy deposits at small angles are observed in several detectors near the outgoing proton beam direction. Particles reach these detectors either directly from the interaction point or indirectly as a result of secondary scattering with the beam pipe wall or adjacent material such as the collimators. The detectors are therefores sensitive to particles well outside their nominal geometrical regions. The liquid argon calorimeter is sensitive to particles with pseudorapidities $\eta = -\ln\tan\theta/2$ up to $\eta \simeq 5.5$. A copper-silicon sandwich calorimeter (PLUG) allows making energy measurements over the range $3.5 < \eta < 5.5$. The three double layers of drift chambers of

the forward muon detector (FMD) are sensitive to particles produced at pseudorapidities $5.0 < \eta < 6.5$. The proton remnant tagger (PRT), consisting of seven double layers of lead/scintillators, located 24 m from the interaction point, covers the region $6.0 < \eta < 7.5$.

1.4 Thrust jet analysis method

The definition of thrust is taken equivalently to [17]. In the centre of mass of a system X of N particles, the thrust method determines the direction of the unit vector $\vec{a}$ along which the projected momentum flow is maximal [18]. Thrust is computed as

$$T = \frac{\max\limits_{\vec{a}} \sum\limits_{j=1}^{N} |\vec{p}_j \cdot \vec{a}|}{\sum\limits_{j=1}^{N} |\vec{p}_j|}, \tag{1.8}$$

where $\vec{p}_j$ represents the momentum of particle j, in the rest of the N particles. Given the thrust axis $\vec{a}$, with an arbitrary directional sense, the N particles can then be grouped into two subsets (thrust jets), depending on whether they belong to the hemisphere with positive or negative momentum component along the thrust axis. The summed particle momenta of hemisphere I form the jet 4-momentum $P_I = \sum_{k=1}^{N_I}$ with N_I the number of particles in hemisphere I, for $I = 1, 2$. The two thrust jets have independent masses, and equal but opposite 3-momenta: $|P_{1,2}| = P$.

Thrust values are always found in the range from the maximum value of $T = 1$ in the case of a 2-particle state or any collinear configuration, to the minimum value of $T = 0.5$ obtained in an isotropic system X with infinite multiplicity. A symmetric 3-particle configuration yields a value $T = 2/3$ and leaves the direction $\vec{a}$ arbitrary in the 3-particle plane, while a non-symmetric topology gives $T > 2/3$ and the thrust axis pointing in the direction of the particle with the highest energy. A non-symmetric 3-particle topology will therefore appear as a 2-jet like configuration with $T < 1$.

In a multihadron state emerging a partonic process, the two back-to-back reconstructed thrust jets are correlated with the hard partons as is described below. In the case of a 2-parton configuration, the thrust value determined from the final state hadron - i. e. at the hadron level - is smaller than 1, and the direction of the thrust axis remains parallel to the direction of the two partons to the extent that the hadrons can be correctly assigned to 'parent-partons'. For an underlying 3-parton system, the reconstructed thrust axis at the hadron level is correlated with the direction of the most energetic parton. This property has been verified to persist down to final state masses $M_X \sim 5\,\mathrm{GeV}$, using $q\bar{q}g$ events from the RAPGAP event generator [19] which includes hadronization and detector effects in the event simulation as well.

A transverse thrust jet momentum P_t can be defined relative to a reference direction $\vec{r}$ as $P_t = P \sin\Theta$ with Θ the angle between $\vec{P}_j$ and $\vec{r}$. In this analysis, the

proton beam direction transformed into the centre of mass frame of the system X is chosen for $\vec{r}$. Since the 4-momentum transfer squared t is small in LRG events, this direction is a good approximation for the $\gamma^*\mathbb{P}$ axis. For $t = t_{\min}$ they are identical. Monte Carlo studies have shown that a diffractive $t - t_{\min}$ distribution with an exponential slope parameter $b = 6\,\mathrm{GeV}^{-2}$ leads to an average smearing of P_t of less than 0.3 GeV. Unlike the γ^* direction, the proton direction in the X rest frame is unaffected by QED-radiation, when calculated from the scattered electron. The $\mathbb{P}$ direction is not well determined experimentally.

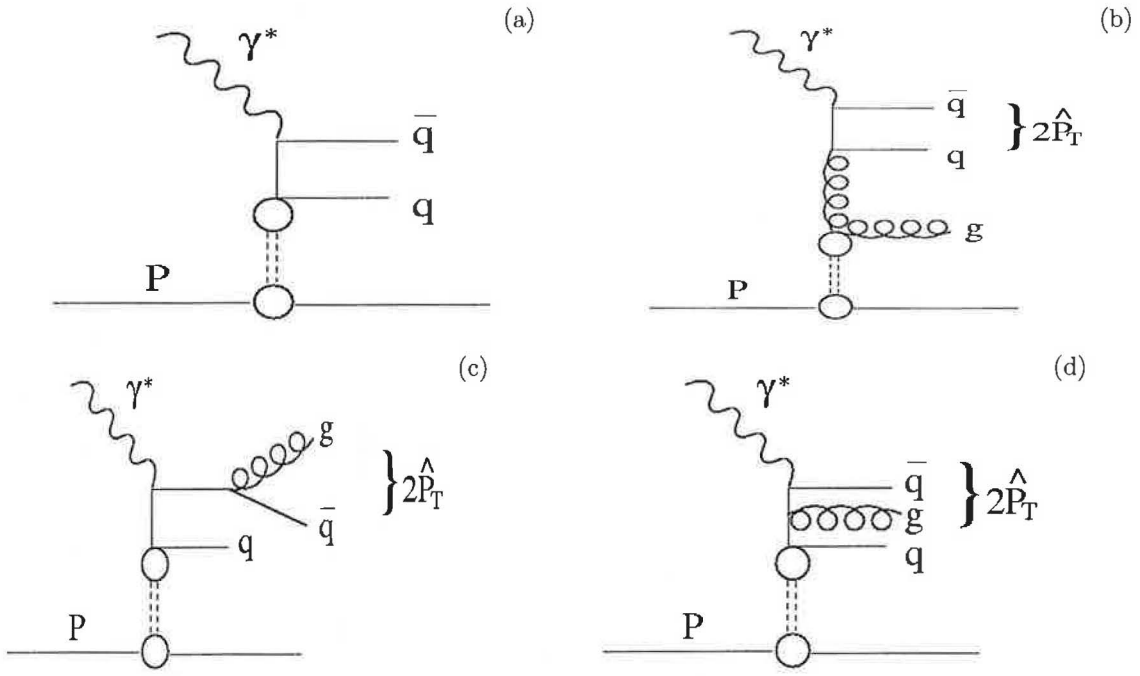

Figure 1.2: Diagrams of parton processes for LRG event: Born term diagram (a), boson-gluon fusion (BGF) (b), QCD-Compton (QCD-C) (c,d).

1.5 Monte Carlo generator RAPGAP

In high energy physics, Monte Carlo Event Generators are used extensively to compare experimental data with theoretical predictions. For example in QCD, the interaction between quarks and gluons can be calculated in leading - or next-to-leading order in the strong coupling constant α_s. In experiments, only stable particles are measured, but not partons (quarks or gluons), which cannot be described by perturbation theory, because the coupling constant α_s becomes large at scales of the order of the mass of hadrons. Thus we have to describe the hadronization phenomenologically.

In the IMF picture, the diagrams in Fig. 1.2 are interpreted as the deep inelastic scattering (DIS) probing a colourless exchange object. This is implemented in the RAPGAP [19] Monte Carlo (MC) program. The RAPGAP model employs deep-inelastic electron scattering off pomerons [14] and off (subleading) reggeons coupling to the proton. The pomeron is ascribed a quark and gluon content. The rations of the BGF to the Born term and to the QCD-C contributions (see Fig. 1.2) depend on the gluon and quark contents of the exchanged objects. These have been determined from QCD analysis with DGLAP evolution [20] of the diffractive structure function measured by the H1 collaboration [21], with the result that most of the pomeron momentum is carried by gluons. For the reggeon, the quark and gluon content is taken to be that of the pion [22].

1.6 HZTool

Data from high-energy physics experiments have seen the triumph of the Standard Model both in precision electroweak measurements and in the verification of QCD to a reasonable degree of precision. However, a number of aspects of high energy collisions remain poorly understood becasuse of the technical difficulties in the calculation. This is particularly the case for measurements of the hadronic final state in high energy collisions, where the specific event shape variables, jet algorithms and kinematic cuts may be rather complex.

Accurate models of the final state are often needed to when designing new experiments and interpreting the data acquired from them. Simulation programs employing fits to existing data address these problems. However, consistent tuning of the parameters of these programs, and examination of the physics assumptions they contain, is non-trivial due to the wide variety of colliding beams, regions of phase space, and complex observables. Comparing a new calculation to a sensible set of relevant data is in practice always extremely time consuming and often leads to various errors.

HZTOOL [23] was created to improve this situation. It is a library of Fortran routines allowing reproduction of the experimental distributions and an easy access to the published data. Basically, each subroutine corresponds to a published paper. If supplied with the final states of a set of simulated collisions, these routines will perform the analysis of the final state exactly as it was performed in the paper, providing simulated data points which may be compared to the measurement. HZTOOL currently contains measurements from ep, γp, $p\bar{p}$ and $\gamma\gamma$ collisions. Others may easily be added.

Chapter 2

Results

The thrust analysis of *ep* diffraction data has been published in 1997 [1] and compared to existing theoretical models. It was found that the average thrust of the final states X, which emerge from the dissociation of virtual photon in the range $10 < Q^2 < 100\,\mathrm{GeV}^2$, grows with hadronic mass M_X and implies a dominant 2-jet topology. Thrust was found to decrease with growing P_t, the thrust jet momentum transverse to the photon-proton collision axis. Distributions of P_t^2 are consistent with being independent of M_X. They show a strong alignment of the thrust axis with the photon-proton collision axis, and have a large high $-P_t$ tail. The correlation of thrust with M_X is similar to that e^+e^- annihilation at $\sqrt{s_{ee}} = M_X$, but with lower values of thrust in the *ep* data. Monte Carlo models RAPGAP and LEPTO were not able to describe the diffraction data [1].

The aim of this analysis is to compare this data to newer version of Monte Carlo model, namely RAPGAP. Using simulated events, the measured distributions in [1] have been corrected for resolution and acceptance losses to give cross sections in a kinematics region defined by

$$M_Y < 1.6\,\mathrm{GeV}, \tag{2.1}$$
$$x_{\mathbb{P}} < 0.05, \tag{2.2}$$
$$|t| < 1\,\mathrm{GeV}^2, \tag{2.3}$$
$$10 < Q^2 < 100\,\mathrm{GeV}^2, \tag{2.4}$$
$$y < 0.5. \tag{2.5}$$

Events with these M_Y, $x_{\mathbb{P}}$ and t limits have large rapidity gap in the detector for kinematics reason.

In our analysis the same sample of cuts as in [1] has been used. The sample of RAPGAP (version 3.01) generated events composes of three files, which correspond to Fig. 1.2 (Born term - two files, and BGF - one file). First two files correspond to structure function of pomeron (uds-pomeron – in Fig. 1.2a, the q substitutes one of the three quarks Up, Down and Strange; and c-pomeron – see Fig. 1.2a, q substitutes quark Charm) and the third one to the structure function of reggeon (uds-meson – see Fig. 1.2b). Absolute and relative (normalized to 1) cross sections

file	σ [nb]	σ_{rel}
uds-pomeron	13.849	0.599
uds-reggeon	7.7136	0.334
c-pomeron	1.5538	0.067

Table 2.1: Absolute and relative cross section for generated files.

of these processes are shown in Tab. 2.1. Errors are negligible because of large statistics of generated events. Each file contains one million of events. In generation procedure the subroutine Hz97210 from HZTool (the number corresponds to the number of DESY preprint where the analysis [1] was published) was used. A lot of histograms was produced from which we were able to create the same plots as in [1] with the help of ROOT program [24], which was made for analysis of physical data.

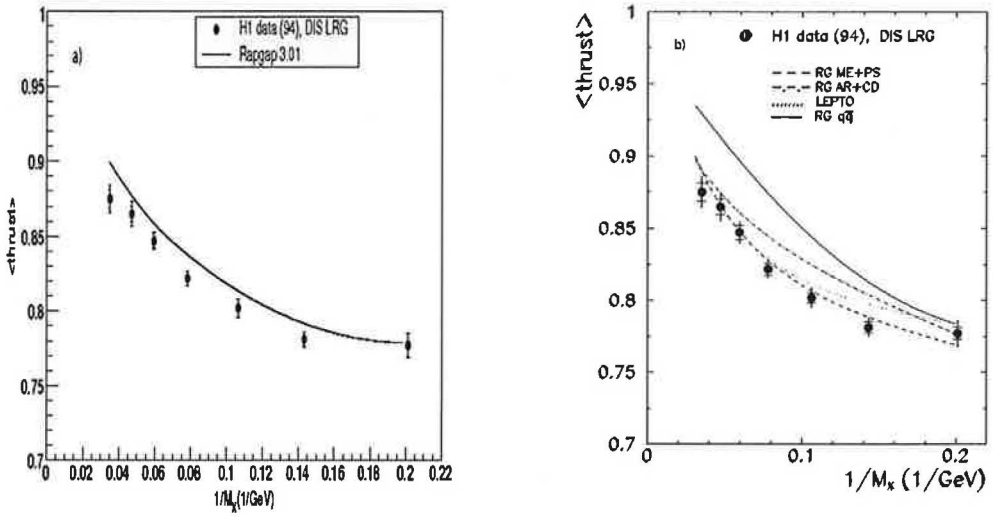

Figure 2.1a: Comparsion of model prediction with the M_X dependence of $\langle T \rangle$; Figure 2.1b: as in a, but with old RAPGAP

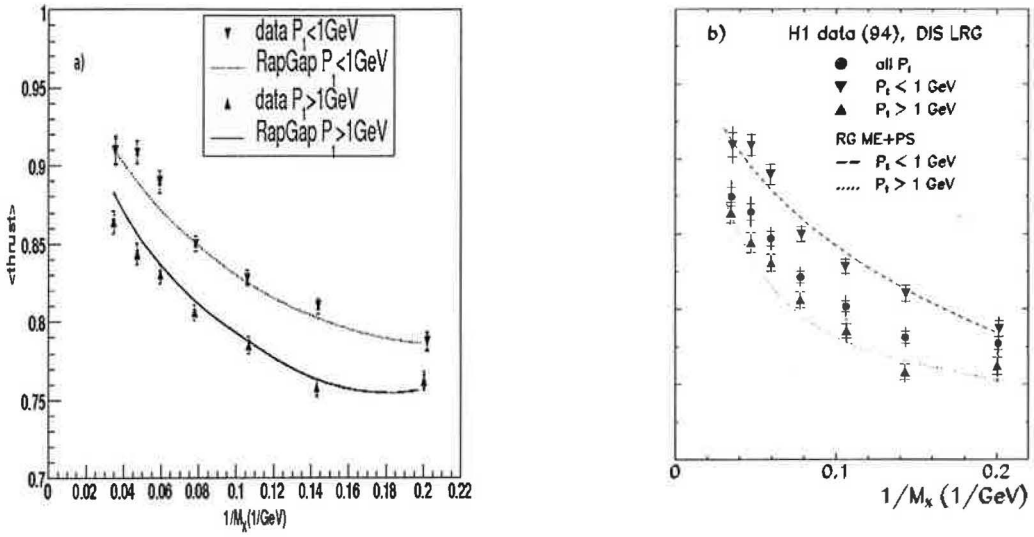

Figure 2.2a: Average thrust $\langle T \rangle$, as a function of $1/M_X$, for events with $P_t < 1\,\mathrm{GeV}$ and for events with $P_t > 1\,\mathrm{GeV}$, with prediction from RAPGAP 3.01; Figure 2.2b: as in a, but with old RAPGAP

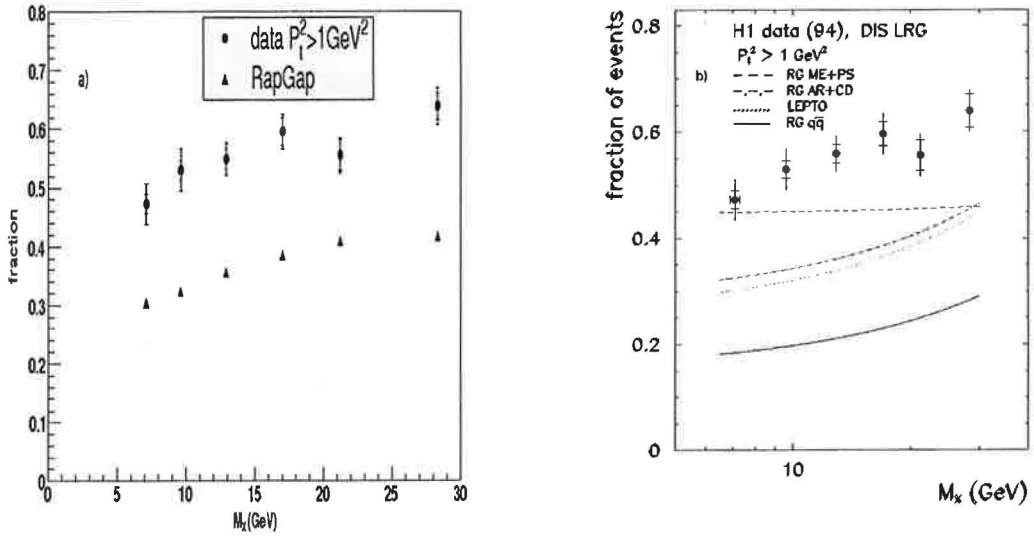

Figure 2.3a: Fraction of events with $P_t^2 > 1\,\mathrm{GeV}^2$ for six M_X intervals, together with RAPGAP prediction; Figure 2.3b: as in a, but with old RAPGAP

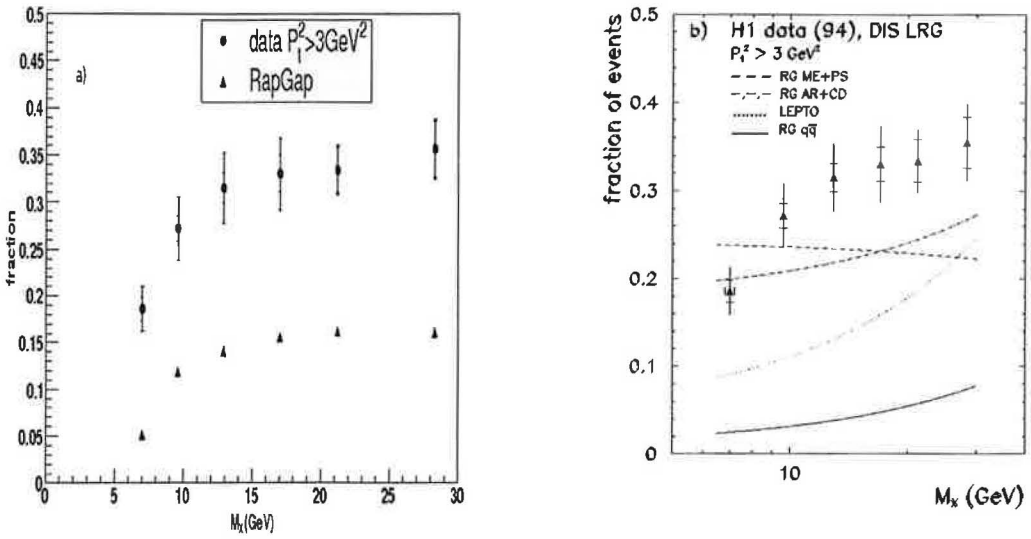

Figure 2.4a: Fraction of events with $P_t^2 > 3\,\mathrm{GeV}^2$ for six M_X intervals, together with RAPGAP prediction; Figure 2.4b: as in a, but with old RAPGAP

The dependence of average thrust $\langle T \rangle$ on the inverted value of mass of system X, $1/M_X$ is qualitavely good described, but with the new version we do not achieve better agreement with experimental data than with the old one (see Fig. 2.1). With the newer version of RAPGAP we obtain slightly larger values of thrust than it is observed for data. It means that generated events have more pencil-like structure than experimental ones.

On Fig. 2.2 the thrust for two samples of data (with $P_t^2 < 1\,\mathrm{GeV}^2$ and $P_t^2 > 1\,\mathrm{GeV}^2$) is shown. Both the old and the newer versions of RAPGAP are able to describe the general features of data.

The fraction of events with $P_t^2 > 1\,\mathrm{GeV}^2$ for six M_X intervals, together with RAPGAP predictions is shown in Fig. 2.3 for old and newer version of RAPGAP. It is evident that the newer version of RAPGAP gives still poor description of data. The same is observed on Fig. 2.4 where the fraction of events but now for $P_t^2 > 3\,\mathrm{GeV}^2$ are shown.

Model RAPGAP clearly underestimates the fractions of events with the large P_t^2 of the thrust jets in comparison with data.

It is evident that model RAPGAP needs still significant improvement to describe properly all the global characteristics of diffractive events.

Chapter 3

Conclusion

The sample of *ep* diffractive events was generated by Monte Carlo generator RAPGAP 3.01 using HZTools subroutine Hz97210. The Monte Carlo distributions for thrust and P_t^2 were compared with the results obtained in [1].

The RAPGAP 3.01 describes the dependence of thrust on mass properly, but there is no evidence of improvement compared to old version of Monte Carlo. The old and the new version of RAPGAP are able to describe as well the value of thrust for two intervals of P_t^2 of data (with $P_t^2 < 1\,\mathrm{GeV}^2$ and $P_t^2 > 1\,\mathrm{GeV}^2$), but there is also no evidence of improvement. Model RAPGAP also clearly underestimates the fractions of events with the large P_t^2 of the thrust jets in comparison with data.

From these studies is it evident that model RAPGAP needs still significant improvement to describe properly all the global characteristics of diffractive events.

Bibliography

[1] H1 Collab., C. Adloff et al., Eur. Phys. J. C1 495-507 (1998).

[2] Feinberg E. L. and Pomeranchuk I. Y.: Suppl. Nuovo Cimento **III**, 652 (1956).

[3] Good M. L. and Walker W. D.: Phys. Rev **120**, 1857 (1960).

[4] Collins P. D.: "An Introduction To Regge Theory And High-Energy Physics," *Cambridge University Press, 1977.*

[5] Gribbov V. N.: JETP Lett. **41**, 667 (1967).

[6] Low F. E.: Phys. Rev. **D12**, 163 (1975).

[7] Nussinov, S.: Phys. Rev. Lett. **34**, 1286 (1975).

[8] Lipatov L. N.: Sov. J. Nucl. Phys. **23**, 338 (1976).

[9] Kuraev E. A., Lipatov L. N. and Fadin V. S.: Sov. Phys. JETP **45**, 199 (1977).

[10] Balitsky I. I. and Lipatov L. N.: Sov. J. Nucl. Phys. **28**, 822 (1978).

[11] Derrick M. *et al.* [ZEUS Collaboration]: Phys. Lett. **B315**, 481 (1993)

[12] Ahmed T. *at al.* [H1 Collaboration]: Nucl. Phys. **B429**, 477 (1994).

[13] Bonino R. *et al.* [UA8 Collaboration]: Phys. Lett. **B211**, 239 (1988).

[14] Ingelman G. and Schlein P. E.: Phys. Lett. **B152**, 256 (1985).

[15] H1 Collab, Abt I. *et al.*: Nucl. Instr. and Meth. **A386**, 310 (1996) and Nucl Instr. and Meth. **A386**, 348 (1996).

[16] H1 BEMC Group, Ban J. *et al.*: Nucl. Instr. and Meth. **A372**, 399 (1996).

[17] Brandt *et al.*: Phys Lett. **12**, 57 (1964).

[18] Farhi E.: Phys. Rev. Lett. **39**, 1587 (1977).

[19] Jung H.: Comp.Phys. Comm. **86**, 147 (1995);
Jung H.: "Modelling Diffractive Processes", Topical Conference on Hard Diffractive Processes, Eilat, Israel, Febr. 1996, p. 406.

[20] Dokshitzer Yu. L.: JETP **46**, 641 (1997);
Gribov V. N., Lipatov L. N.: Sov. Journ. Nucl. Phys. **15**, 78 (1972);
Altarelli G., Parisi G.: Nucl. Phys. **B126**, 298 (1972).

[21] H1 Collab., A. Aktas et al, Eur. Phys. J.: C48, 715, 2006.

[22] Glück M., Reya E. and Vogt A.: Z. Phys. **C53**, 651 (1992)

[23] HZTool package, manual and tutorial can be downloaded from `http://hepforge.cedar.ac.uk/hztool/`

[24] Root home page `http://www.root.cern.ch`